J. Phys. A: Math. Gen. **29** (1996) 7739–7755. Printed in the UK

# Phase transitions and critical behaviour in one-dimensional non-equilibrium kinetic Ising models with branching annihilating random walk of kinks

Nóra Menyhárd† and Géza Ódor‡

† Research Institute for Solid State Physics, H-1525 Budapest, PO Box 49, Hungary
‡ Research Institute for Materials Science, H-1525 Budapest, PO Box 49, Hungary

Received 27 June 1996, in final form 5 September 1996

**Abstract.** One-dimensional non-equilibrium kinetic Ising models evolving under the competing effect of spin flips at zero temperature and nearest-neighbour spin exchanges exhibiting a parity-conserving (PC) phase transition on the level of kinks are now further investigated numerically, from the point of view of the underlying spin system. Critical exponents characterizing its statics and dynamics are reported. It is found that the influence of the PC transition on the critical exponents of the spins is strong and the origin of drastic changes as compared to the Glauber–Ising case can be traced back to the hyperscaling law stemming from directed percolation. The effect of an external magnetic field, leading to directed percolation-type behaviour on the level of kinks is also studied, mainly via the generalized mean-field approximation.

## 1. Introduction

Non-equilibrium phase transitions have attracted great interest lately. A variety of sytems studied seem to belong to the universality class of directed percolation (DP) [1–4]. The DP universality class is very robust. Among transitions that belong to it are the transitions in branching annihilating random walk (BARW) models with an odd number of offsprings in the process $A \to A + nA$ [5–7]. Numerical studies by Grassberger and von der Twer [8, 9] of probabilistic cellular automata models in one dimension involving the processes $k \to 3k$ and $2k \to 0$ ($k$ stands for kink) have revealed, however, a new universality class of dynamic phase transitions. Both time-dependent and steady-state simulations have resulted non-DP values for the relevant critical exponents. This so-called parity-conserving (PC) phase transition has since been found in a variety of models. The $n = 4$ BARW model has been studied in the greatest detail and accuracy by Jensen [10]. In a previous paper [11] one of the the authors has introduced a family of non-equilibrium kinetic Ising models (NEKIM) showing the same phenomenon, while quite recently, with an appropriate modification of the original BARW model (suggested already in [11]), the $n = 2$ BARW model has been shown to exhibit the PC transition as well [12]. The two-component interacting monomer–dimer model introduced by Kim, Park and Park [13–15] represents a more complex sytem with a PC-type phase transition.

Formerly, combinations of Glauber [16] and Kawasaki [17] kinetics were introduced with the aim of investigating temperature-driven non-equilibrium phase transitions [18, 19]. In [11], however, spin-flip kinetics was taken at $T = 0$ alternating with random nearest-neighbour spin exchanges (Kawasaki-exchange at $T = \infty$). The mean-field limit of this

0305-4470/96/237739+17$19.50  

model together with results of the generalized mean-field theory (GMF) have been presented in [20].

In the present paper we further investigate NEKIM but now from the point of view of the underlying 1D spin system with the aim of getting some more insight into the nature of the PC transition. Results of computer simulations are presented for different critical exponents connected with the structure factor. The new computational technique based on short-time dynamics and finite-size scaling, as introduced and applied by Li *et al* [21, 22] for calculating moments of the magnetization and the time-dependent Binder cumulant [23], is also applied here besides the usual finite-size scaling (FSS) and time-dependent simulations. In all our numerical studies the initial state is random with zero magnetization and concerning finite-size effects the use of antiperiodic boundary conditions instead of the usual periodic ones will prove to be essential.

In the field of domain-growth kinetics it has long been accepted that the scaling exponent of $L(t)$, the characteristic domain size, is equal to $\frac{1}{2}$ if the order parameter is non-conserving. Now let us restrict ourselves to a 1D Ising spin chain of length $L$ and define the structure factor at the ferromagnetic Bragg peak as usual: $S(0,t) = L[\langle M^2\rangle - \langle M\rangle^2]$, $M = \frac{1}{L}\sum_i s_i$, ($s_i = \pm 1$). If the conditions of validity of scaling are fulfilled [24] then

$$S(0,t)) \propto [L(t)]^d \qquad L(t) \propto t^x \tag{1}$$

where now $d = 1$ and $x = \frac{1}{2}$. Another quantity usually considered [24] is the excess energy $\Delta E(t) = E(t) - E_T$ ($E_T$ is the internal energy of a monodomain sample at the temperature of quench), which in our case is proportional to the kink density $n(t) = \frac{1}{L}\langle\sum_i \frac{1}{2}(1-s_i s_{i+1})\rangle$:

$$n(t) \propto \frac{1}{L(t)} \propto t^{-y} \tag{2}$$

with $y = \frac{1}{2}$ in the Glauber–Ising case, expressing the well known dependence on time of annihilating random walk.

It is also well known, that near zero temperature the parameter $p_T = \mathrm{e}^{-4J/kT}$ can be regarded as the quantity measuring the deviation from the critical temperature $T_c = 0$ of the 1D Ising model, and the usual (equilibrium) critical exponents can be defined as powers of $p_T$. From exact solutions, keeping the leading order terms for $T \to 0$, the critical exponents of ($k_B T$ times) the spin-susceptibility, coherence length $\xi$ and the magnetization are known to be $\gamma = \nu = \frac{1}{2}$, $\beta = 0$, respectively. Fisher's static scaling law $\gamma = d\nu - 2\beta$ is valid. Moreover, the dynamic critical exponent $Z$, defined through the relaxation time $\tau$ of the order parameter near $T = 0$ as $\tau = \tau_0 \xi^Z$, is equal to 2.

Instead of Glauber kinetics, let us now apply the non-equilibrium NEKIM kinetics, and investigate the Ising system at and in the immediate neighbourhood of one of its PC points. On the level of kinks the PC point, separating the active and absorbing phases, is a second-order transition point, while from the point of view of spins the absorbing phase consists of a multitude of 1D Ising critical points, which ends at the PC point. We are interested in the behaviour of the spin system at this end-point.

The result is the following. The critical kink-dynamics has a strong influence on the spin-kinetics and even on its statics. Domain growth is governed by criticality: $x = 1/Z$, but the dynamic exponent $Z$ changes from $Z = 2$ to $Z = 1.75$. As to statics, $\gamma = \nu = 0.444$ while $\beta = 0$ and Fisher's scaling law remains valid.

More spectacular is the change of the above $y$-exponent: $y = x/2$; $x = 0.57$ and similarly the exponent $\alpha_n$ of the finite-temperature kink-density, $\lim_{t\to\infty} n(t, p_T) \propto {p_T}^{\alpha_n}$, which is $\frac{1}{2}$ in the Glauber–Ising limit, decreases to $\alpha_n = \gamma/2 = 0.222$. We shall argue that this factor of 2 between magnetic-and kink-exponents has its origin in the hyperscaling

law, introduced for DP by Grassberger and de la Torre [1], which connects exponents of time-dependent kink density and cluster-size.

These numerical results will be reported in detail in the following. Moreover, we shall present further results, mainly from the viewpoint of applying GMF approximations, by introducing a magnetic field term into the spin-flip probability, which causes the PC transition to become DP-like [15].

## 2. The model

The model we will investigate here is a one-dimensional kinetic Ising model evolving by a combined spin-flip and spin-exchange dynamics as described in [11]. The spin-flip transition rate in one-dimension for spin $s_i$ sitting at site $i$ is

$$w_i = \frac{\Gamma}{2}(1 + \delta s_{i-1}s_{i+1})\left(1 - \frac{\gamma}{2}s_i(s_{i-1} + s_{i+1})\right) \tag{3}$$

where $\gamma = \tanh 2J/kT$ ($J$ denoting the coupling constant in the Ising Hamiltonian), $\Gamma$ and $\delta$ are further parameters. While in [11] $T = 0$ ($\gamma = 1$) has been taken, we shall consider now finite-temperature effects, too. Instead of $\gamma$ the parameter $p_T$ will be used in the following. The three independent rates

$$w_{indif} = \frac{\Gamma}{2}(1 - \delta) \qquad w_{oppo} = \Gamma(1 + \delta)\frac{1}{1 + p_T} \qquad w_{same} = \Gamma(1 + \delta)\frac{p_T}{1 + p_T} \tag{4}$$

where the subscripts of $w$ refer to the three possible neighbourhoods of a given spin, are responsible—on the level of domain walls—for random walk, annihilation and pairwise creation (inside of a domain) of kinks, respectively.

The other ingredient of NEKIM has been a spin-exchange transition rate of neighbouring spins (the Kawasaki [17] rate at $T = \infty$):

$$w_{ii+1} = \tfrac{1}{2}p_{ex}[1 - s_i s_{i+1}] \tag{5}$$

where $p_{ex}$ is the probability of spin exchange.

Spin-flip and spin-exchange have been applied alternatingly at each time step, the spin-flip part has been applied using two-sublattice updating, while making $L$ MC attempts at random ($L$ denotes the size of the chain) has been counted as one time-step of exchange updating. In this system, at $T = 0$, a PC-type phase transition takes place. In [11] we have started from a random initial state and determined the phase boundary in the ($\delta$, $pex$) plane. In the following we will choose a typical point on this phase diagram and make simulations at and around this point, fixing $\Gamma$ and $p_{ex}$ and changing only $\delta$. The parameters chosen are: $\Gamma = 0.35$, $pex = 0.3$, $\delta_c = -0.395(2)$. We note here that $\Gamma$ appeared as $1/\Gamma$ in [11] and $\delta_c$ has a more accurate value now than previously.

## 3. Scaling forms and laws

In the following we will be interested in two quantities characterizing the behaviour of the NEKIM, namely the structure factor or spin-susceptibility and the kink-density under the conditions of a quench. Thus, in contrast to to the usually considered evolution from a pair of kinks, we will restrict ourselves to completely random initial states ($T = \infty$, $M(0) = 0$) and follow the development of the system via the rules described in the previous section. With $p_T$ defined above and $\epsilon = |\delta - \delta_c|$, where $\delta < 0$ is the parameter which drives the

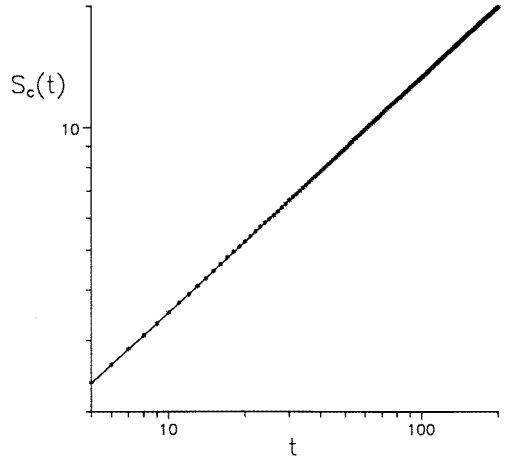


**Figure 1.** The structure factor as a function of time at a typical phase transition point of the NEKIM phase diagram. $L = 128$, and the number of independent initial configurations with zero magnetization, was $10^5$. Here $t_{max} = 200$ and finite-size effects start to set in at about $t = 1000$. The straight line is the fit with $x = 0.570$.

phase transition in the present case, the scaling forms for $S$ and $n$ are as follows:

$$S(p_T, \epsilon, L, t) = t^x f\left(\frac{t^{\frac{1}{Z_c}}}{\xi}\frac{t^{\frac{1}{Z}}}{\xi_\perp}, \frac{\xi}{L}, \frac{\xi_\perp}{L}\right) \tag{6}$$

$$n(p_T, \epsilon, L, t) = t^{-y} g\left(\frac{t^{\frac{1}{Z_c}}}{\xi}\frac{t^{\frac{1}{Z}}}{\xi_\perp}, \frac{\xi}{L}, \frac{\xi_\perp}{L}\right) \tag{7}$$

with $\xi = {p_T}^{-\nu}$, $\xi_\perp = \epsilon^{-\nu_\perp}$. The exponents connected with $\epsilon$ have been written using the notation of directed percolation, while those related to the temperature factor $p_T$ are written in the notation of equilibrium Ising system. $Z$ and $Z_c$ are the respective dynamic critical exponents and we allow for the possibility that they differ (though this will turn out not to be the case). We note here that the exponent $y$ used to be called $\alpha$ in [11].

### *3.1. The large-L case*

Let us first take the limit $L \to \infty$. Then the dependences on $\xi/L$ and $\xi_\perp/L$ can be neglected in equations (6) and (7). If, furthermore, $\xi \to \infty$, $\xi_\perp \to \infty$ the forms valid at the critical point $\epsilon = 0$, $p_T = 0$ are obtained: $S_c(t) \propto t^x$ and $n_c(t) \propto t^{-y}$. Figure 1 shows $S_c(t) \propto t^x$, with the result $x = 0.570(1)$. The data yield $y = 0.285(1)$ for the kink density decay exponent. It is worth noticing that within the errors, $x = 2y$. We have also made simulations for the same quantities with $L = 8000$ up to $t = 3 \times 10^4$ and averaging over 2000 initial states with similar result but with higher error and more than 100 times greater computer time.

Keeping $p_T = 0$, near $\delta_c$ in the active phase, equation (7) gives, for $t \to \infty$, the order parameter $n(\epsilon) \propto \epsilon^{\beta_n}$ with the scaling law[9]

$$\beta_n = \nu_\perp Z y. \tag{8}$$

A similar scaling relation can be obtained from (6), which yields for $t \to \infty$: $S(\epsilon) \propto \epsilon^{-\Theta}$ with

$$\Theta = \nu_\perp Z x. \tag{9}$$

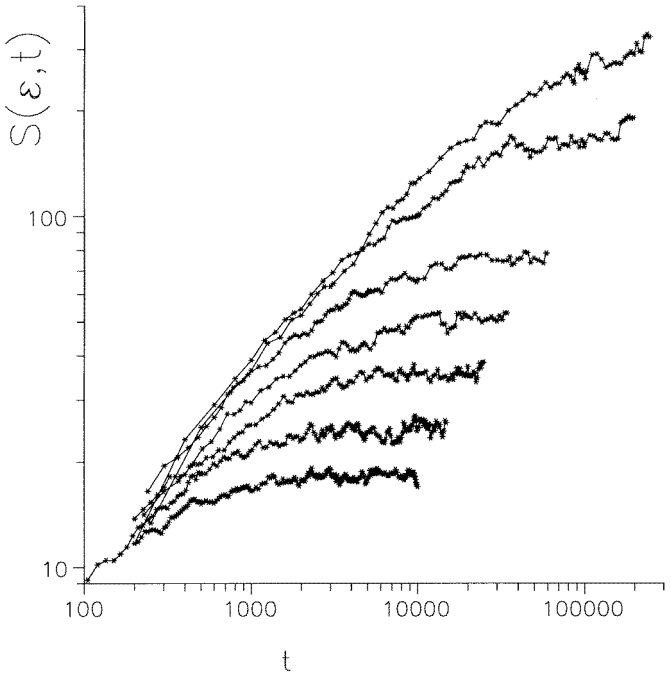


**Figure 2.** The structure factor $S(\epsilon, t)$ in the active phase in the vicinity of the PC transition point for the following values of $\epsilon$: 0.13, 0.11, 0.09, 0.075, 0.06, 0.04, 0.03 (from bottom to top). $L$ was varied between 2000 and 8000 to avoid finite-size effects before saturation sets in. The number of independent states in averaging is typically 1000.

The divergence of the spin-susceptibility as a function of $\epsilon$ is understandable: in the subcritical regime (i.e. for $|\delta| < |\delta_c|$ ) it is infinite ( $T \to 0, t \to \infty$), because the whole subcritical region is a plane of 1D critical (Ising) points. In order to get $\Theta$ directly, we have made simulations for $S(\epsilon, t)$ around the chosen PC point in the interval $\epsilon = 0.02$–$0.13$ as shown in figure 2. The (time-averaged) saturation values of $S$ yield the exponent $\Theta = 1.9(1)$. From the same runs as above we have now obtained $\beta_n = 0.88(4)$. Thus within the errors $\Theta = 2\beta_n$, a relation which also follows from equations (8) and (9) with $x = 2y$. It is worth noting here that on the basis of the divergence of the spin-susceptibility, $S(\epsilon)$, the PC transition point (as end-point of a line of first-order transitions) can be found, without any reference to kinks.

Taking now $\epsilon = 0$ and keeping $p_T$ finite in the limit $t \to \infty$ we get from equation (7) $n(p_T) \propto {p_T}^{\alpha_n}$ and the scaling relation

$$\alpha_n = y\nu Z_c. \tag{10}$$

Figure 3 shows $n(t, p_T)$ as a function of $t$ at different values of $p_T$ at $\epsilon = 0$; the level-off values could be fitted with $\alpha_n = 0.222(5)$. This result is in accord with the value for the $n = 4$ BARW reported by Jensen [10] ($1/\delta_h$ in his notation).

Similarly, taking equation (6) at $\epsilon = 0$ and in the limit $t \to \infty$ the spin-susceptibility arises: $\chi \propto {p_T}^{-\gamma}$ together with the scaling relation

$$\gamma = x\nu Z_c. \tag{11}$$

In figure 4 $S(p_T, 0, t)$ is plotted for different values of $p_T$. The temperature-dependent simulations have been performed in the range $p_T = 1 \times 10^{-1}$–$5 \times 10^{-5}$. The level-off values

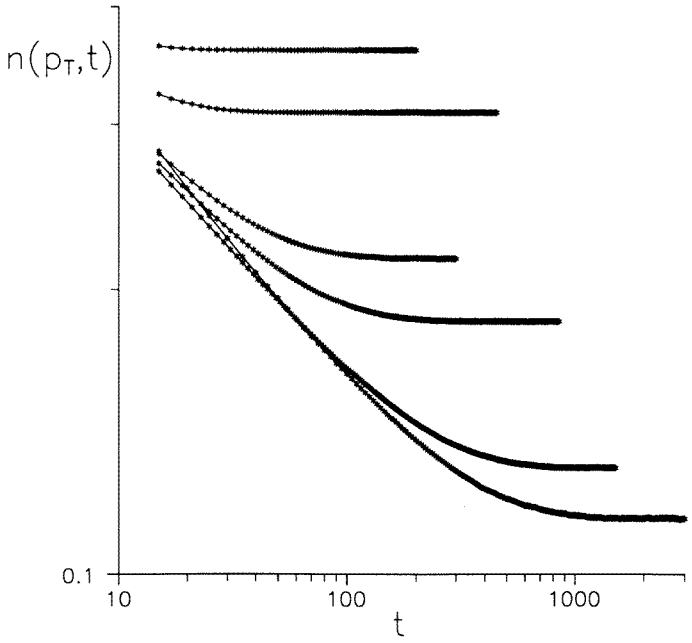


**Figure 3.** The kink-density as a function of temperature and time $n(p_T, t)$. The curves are for $p_T = 10^{-1}, 5.0 \times 10^{-2}, 10^{-2}, 5.0 \times 10^{-3}, 10^{-3}, 5.0 \times 10^{-4}$ from top to bottom. $L = 2000$ and the number of samples in averaging is typically $2 \times 10^4$.

seen in figure 5, where the data for the two highest temperatures ($p_T = 1 \times 10^{-1}, 5 \times 10^{-2}$) were discarded, yield the exponent of the spin-susceptibility at the PC point as $\gamma = 0.445(5)$. This value is in accord, within errors, with the scaling laws (10) and (11) which predict, using the relation $x = 2y$ found above, $\gamma = 2\alpha_n = 0.444$.

It is to be noted that due to the non-self-averaging property of the structure factor [25], all exponents connected with this quantity have much larger statistical errors than the ones connected with the kink density, and the same applies to the time-dependent simulations. This explains the large fluctuations exhibited on figures 2 and 4 in comparison with e.g. figure 3.

### *3.2. Static finite-size scaling*

Finite-size scaling will be used to find numerical values for some more exponents. The static FSS limit requires to take first the limit $t \to \infty$ and to suppose $L \ll \xi, \xi_\perp$. Let us consider now the two possible orders of limits to reach the PC point: (a) $p_T = 0$, $\epsilon \to 0$ and (b) $\epsilon = 0$, $p_T \to 0$.

*Case (a).* Equations (6) and (7) lead to the expressions

$$\lim_{\epsilon \to 0} S(\epsilon, L) = L^{\Theta/\nu_\perp} f''(L/\xi_\perp) \propto L^{\Theta/\nu_\perp}$$

and

$$\lim_{\epsilon \to 0} n(\epsilon, L) = L^{-\beta_n/\nu_\perp} g''(L/\xi_\perp) \propto L^{-\beta_n/\nu_\perp}$$

respectively.

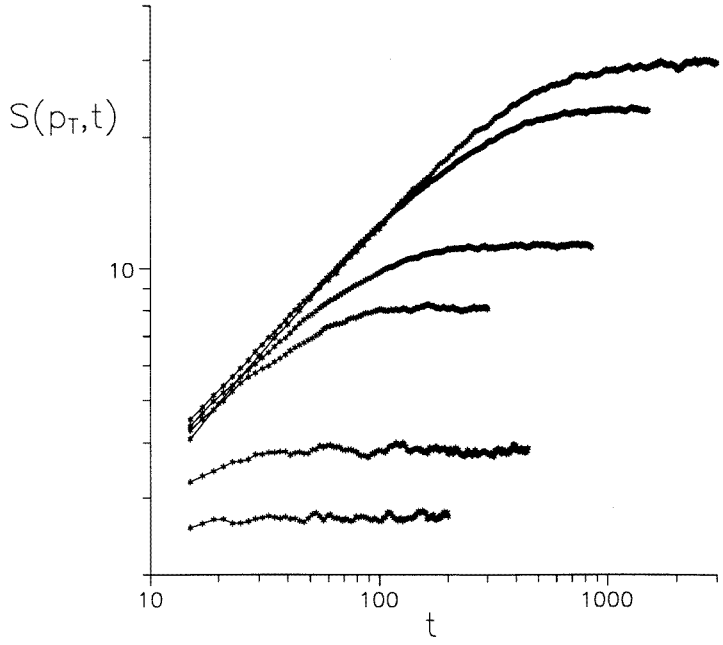


**Figure 4.** The structure factor $S(p_T, t)$ for different values of $p_T$. Details of simulation is as figure 3 except that $p_T$ is decreasing from bottom to top here.

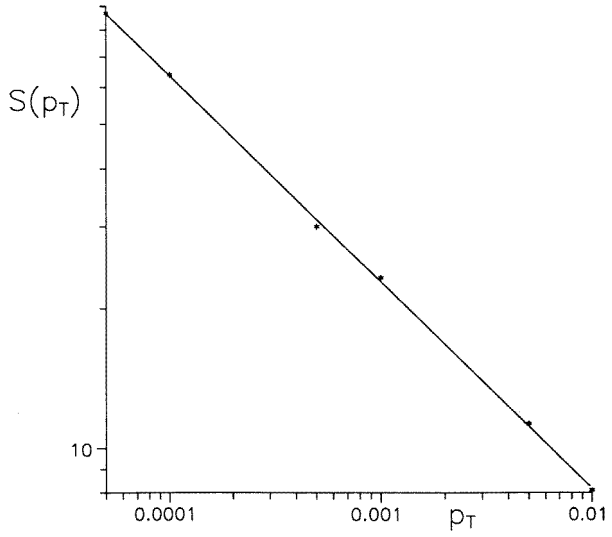


**Figure 5.** The saturation values of figure 4 time-averaged, on a double-logarithmic scale. Data for $p_T = 10^{-4}, 5 \times 10^{-5}$, not shown on figure 4, have also been included. Straight line: fit of data points with $\gamma = 0.445$.

*Case (b).* From equations (6) and (7) we now get

$$\lim_{p_T \to 0} S(p_T, L) = L^{\frac{\gamma}{\nu}} \tilde{f}''(L/\xi) \propto L^{\frac{\gamma}{\nu}}$$

and

$$\lim_{p_T \to 0} n(p_T, L) = L^{-\alpha_n/\nu} \tilde{g}''(L/\xi) \propto L^{-\alpha_n/\nu}$$

respectively.

Within errors we have not found any (numerical) evidence against the supposition that the order of limits $\epsilon \to 0$ and $p_T \to 0$ were interchangeable. The same fixed point seems to be reached in both cases. (Actually this fact has expressed itself already in our finding, according to which the time-exponents $x$ and $y$ are also the same, independently from where we approach the limit $\epsilon = 0$, $p_T = 0$; the difference should have been seen in the pre-asymptotic time dependence. For very small values of, for example, $p_T$ at $\epsilon = 0$, $x = 0.57$, $y = 0.28$ was always clearly seen in the early-time behaviour of $S(t)$ and $n(t)$, respectively).

Thus the above relations lead to the following scaling equalities:

$$\frac{\gamma}{\nu} = \frac{\Theta}{\nu_\perp} \qquad \frac{\beta_n}{\nu_\perp} = \frac{\alpha_n}{\nu}. \tag{12}$$

In numerical simulations with random initial states usually periodic boundary conditions (PBC) are supposed. The fact that PBC allow only an even number of kinks does not matter except under the conditions of FSS close to the PC point, as eventually for all samples the ordering becomes perfect (depletion of kinks) and trivially $\gamma/\nu = \Theta/\nu_\perp = 1$. Because of the same reason it is not possible to find the $L$-dependence of the kink density, which breaks down as a function of time. The proper procedure is to use antiperiodic boundary conditions (APBC), a choice which allows only an odd number of kinks (i.e. all samples are surviving) provided the updating procedure is carefully done. As in the course of dynamic FSS one reaches fixed points, which coincide with the limiting values ($t = \infty$) of $S$ and $n$ above; we will cite our results in the next section.

As we shall see $\gamma/\nu = 1$ is also valid in the case of antiperiodic boundary conditions, which value, together with equation (11), gives $Z_c = 1/x$. Moreover, we shall arrive at $\beta_n/\nu_\perp = \frac{1}{2}$ which, using equations (8) and (9), gives $\Theta/\nu_\perp = 1$ and leads to $Z = 1/x$. Thus $Z_c = Z$, and the two critical dynamical exponents coincide, as anticipated. It is worth noting that the $Z = 1/x$-type relation between the dynamic critical exponent and the domain growth exponent has been found earlier for various 1D equilibrium Ising systems [26].

### *3.3. Early-time dynamic Monte Carlo method*

In the case of systems quenched to their critical temperature [27] universality and scaling may appear in quite an early stage of time evolution, far from equilibrium, where $\xi$ is still small. Based on the scaling relation for such early time intervals, a new way for measuring static and dynamic exponents has been proposed [23, 21, 22]. Now we apply this method to get critical exponents for a non-equilibrium phase transition.

Following [21, 22] we shall suppose the following relation to hold for the $k$th moment of the magnetization near the critical point of the 1D spin system:

$$M^{(k)}(t, p_T, L) = b^{-k\beta/\nu} M^{(k)}(b^{-Z} t, b^{1/\nu} p_T, b^{-1} L) \tag{13}$$

where zero initial magnetization has been considered, and $b$ is a rescaling factor ($b = 2$ will be chosen). After generating randomly an initial configuration, the system is allowed to evolve according to the non-equilibrium kinetic rule of section 2 at $p_T = 0$. (We could have included $\epsilon$ in equation (13) as well, but we will restrict ourselves to the case $\epsilon = 0$, $p_T = 0$, so it is of no importance here.) An average is taken over the initial configurations

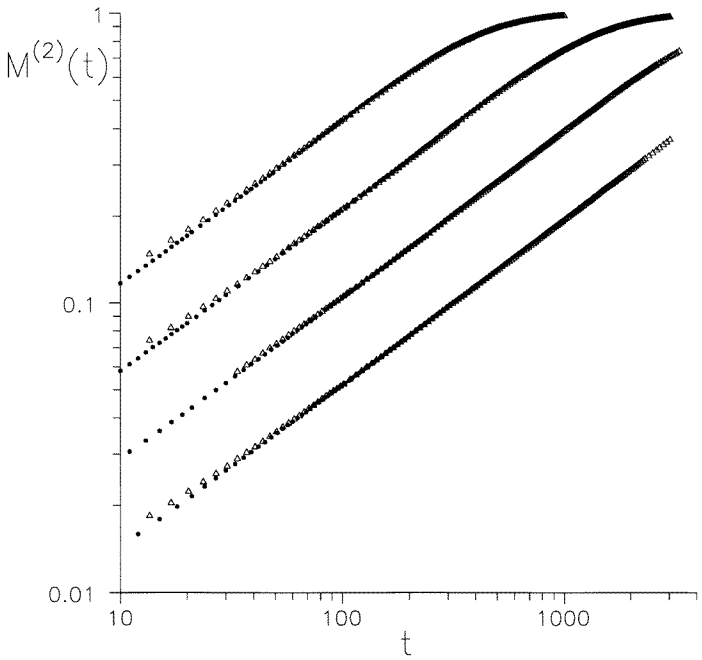


**Figure 6.** Collapsing of curves for $M^{(2)}$ with periodic boundary conditions on a double-logarithmic scale. △: rescaled data; ●: original data. From top to bottom: $L = 16$ (△), 32 (●); 32 (△), 64 (●); 64 (△), 128 (●); 128 (△), 256 (●). The number of samples with random initial states in the averaging was typically $10^5$.

with zero magnetization. In order to get sufficiently good statistics averaging has to be performed over very many ($10^5$–$10^6$) independent initial states, as emphasized by Li *et al* [21, 22] who applied the method to the 2D Ising model. To get the dynamical exponent $Z$ with great accuracy, they proposed calculation of the time-dependent Binder cumulant:

$$U(t, p_T, L) = 1 - \frac{M^{(4)}}{3(M^{(2)})^2} \tag{14}$$

which behaves at $p_T = 0$ as

$$U(t, 0, L) = U(b^{-Z}t, 0, L/b). \tag{15}$$

Similarly to equation (13), but now on the level of kinks, the following relation can be written for $n(t, L)$:

$$n(t, L) = b^{-\beta_n/\nu_\perp} n(b^{-Z}t, b^{-1}L). \tag{16}$$

Note that equation (16) contains $\beta_n$, $\nu_\perp$ and not $\beta$, $\nu$.

Considering the spin system first, besides the triviality of the fixed points reached ($M^{(2)*} = 1$, $U^* = \frac{2}{3}$) the PBC case still leads—by proper fitting—to the value of $Z$ and $\beta$. In case of $M^{(2)}$, using equation (13), collapsing of curves for different values of $L$ has lead to $\beta = 0.00(2)$, $Z = 1.75(2)$; see figure 6. In the case of $U(t, 0, L)$, which contains only $Z$ as a fitting parameter and thus provides it directly, collapsing of curves could again be achieved with $Z = 1.75(1)$. Typically $10^5$–$3 \times 10^5$ averages have been performed. With antiperiodic boundary conditions, collapse of curves has led us to the same results as above

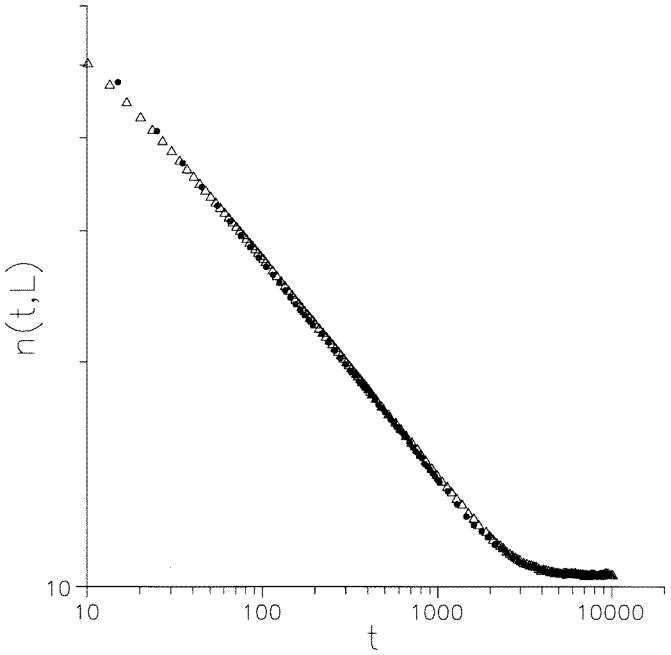


**Figure 7.** Collapsing of curves for $n(t, L)$ according to equation (16). △: $L = 100$, rescaled; ●: $L = 200$. Number of samples in the averaging: $10^5$. Boundary condition: antiperiodic; scale: double-logarithmic.

concerning the exponents $\beta$ and $Z$. Under these conditions, however, important additional information arises from best fit to time-averaged saturation values.

Concerning the kink density $n(t, L)$, equation (16), the collapse of curves is illustrated with $L = 100, 200$ in figure 7. The curves scale together with $Z = 1.75(1)$ and $\beta_n/\nu_\perp = 0.52(2)$. On the other hand, fitting the time-averaged saturation values for $L = 50, 64, 100, 128, 200, 256$ gives for the kink-density $n(L) = 0.66 \times L^{-0.48(2)}$. Thus we conclude that $\beta_n/\nu_\perp\ (= \alpha_n/\nu) = 0.50(2)$. This is in accord with the result of Jensen for the $n = 4$ BARW [10]. In figures 8 and 9, respectively, $M^{(2)}$ and $U$ are seen with antiperiodic boundary conditions for some values of $L$. It is apparent that $U$ is much more sensitive: even here many more samples in averaging would have been needed to smooth out the curves. The time-averaged saturation values for $L = 50, 64, 100, 128, 200, 256$ lead to $S(L) = 0.26L^{0.99(1)}$ (figure 10), thus $\gamma/\nu\ (= \Theta/\nu_\perp) = 0.99(1)$. The difference as compared with the PBC case shows up in the prefactor (0.26(1) instead of 1.0). For the Binder cumulant $U^* = 0.32(1)$, again differing from the PBC value of $\frac{2}{3}$. For the sake of comparison, we have carried out the same kind of simulations for the Ising–Glauber case ($p_{ex} = 0, \delta = 0$) with APBC, and obtained $M^{(2)*}_{Gl} = 0.333(3)$, $n^*{}_{Gl} = 1.00(5)/L$, $U^*{}_{Gl} = 0.40(1)$. Here $Z = 2$ and $\beta = 0$ have given the best fit and similar result can be expected in the whole absorbing phase. It is worth mentioning here that these fixed-point values can be derived exactly for the Glauber case with the result: $M^{(2)*}_{Gl} = \frac{1}{3}$, $n^*{}_{Gl} = 1/L$, $U^*{}_{Gl} = 0.4$ [28].

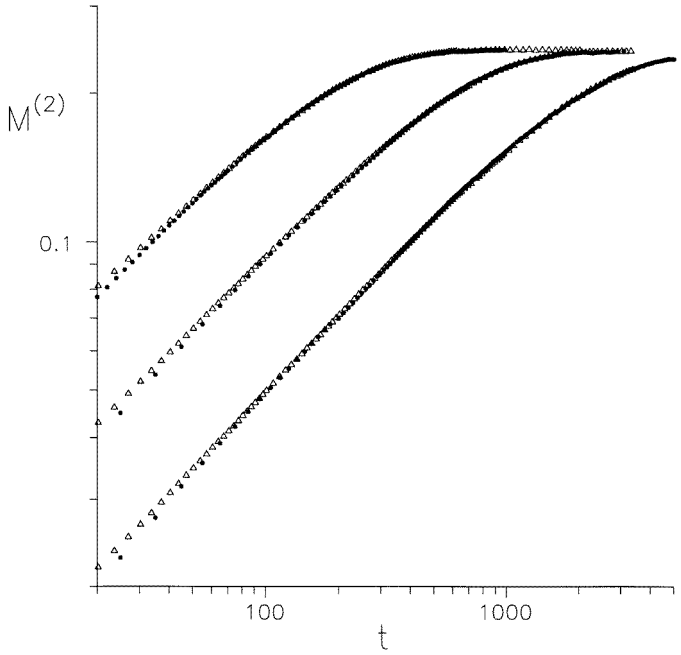


**Figure 8.** $M^{(2)}(t, L)$ with APBC. Rescaling with $b = 2$, $\beta = 0$ and $Z = 1.75$ has resulted in data points marked by △. Collapsing of curves is shown, from top to bottom, for $L = 32$ (△), 64 (●); 64 (△), 128 (●); 128 (△), 256 (●). Number of samples in averaging: $10^5$–$3 \times 10^5$.

## 4. Symmetry-breaking field

It is by now well established that the PC transition has non-DP critical exponents, because of the modulo 2 conservation law. Park and Park [15] have introduced a symmetry breaking external field in case of the interacting monomer–dimer model and showed that the DP universality class is recovered if one of the absorbing states is singled out. They have also mentioned having similar, though—to our knowledge—not yet published data for NEKIM and Grassberger's automata. We have investigated the effect of an external magnetic field $H$ on the NEKIM model with simulations and with the help of the generalized mean-field (GMF) technique as well, both confirming the DP behaviour. The transition probabilities of NEKIM, as given in section 2, are modified in the presence of en external magnetic field $H$ as:

$$w^h_{indif} = w_{indif}(1 - hs_i) \tag{17}$$

$$w^h_{oppo} = w_{oppo}(1 - hs_i) \tag{18}$$

$$h = th\left(\frac{H}{kT}\right) \qquad p_T = 0. \tag{19}$$

Figure 11 shows the phase diagram of NEKIM in the $(h, \delta)$ plane, starting at the reference PC point for $h = 0$ used in this paper ($\delta_c = -0.395$). We have applied only random initial state simulations to find the points of the line of phase transitions (critical exponents: $y = 0.17(2)$, $\beta_n = 0.26(2)$). It is seen, that with increasing field strength the critical point is shifted to more and more negative values of $\delta$.

As to the treatment of the model with the use of the GMF technique, the details of which

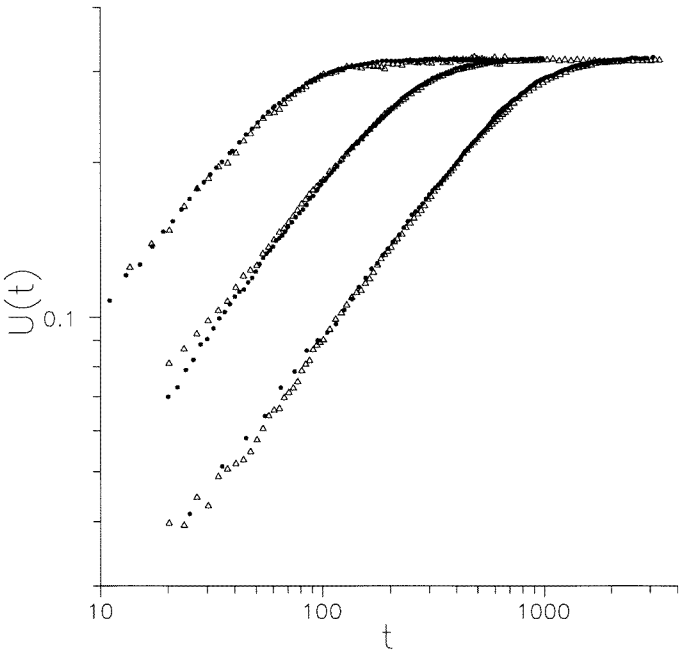


**Figure 9.** $U(t, L)$ with APBC for $L = 16$ (△), 32 (●); 32 (△), 64 (●); 64 (△), 128(●) (from top to bottom). Best collapse of curves again with $Z = 1.75$. Number of samples in averaging: as for figure 8.

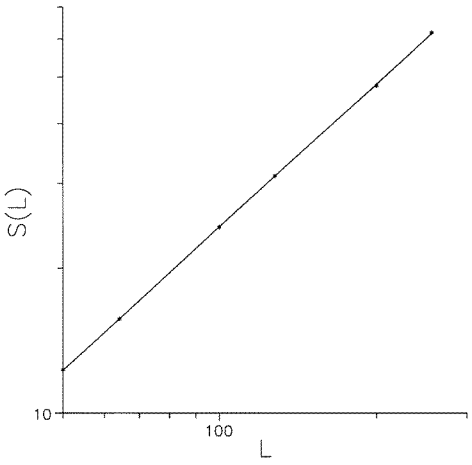


**Figure 10.** Time-averaged saturation values $S(L)$ of $M^{(2)}(t, L)$ shown on a double-logarithmic scale. Straight line: power-law fit with $\gamma/\nu = 0.99$. Averaging has been performed over $10^5$–$3 \times 10^5$ independent random initial states with APBC.

have been explained in [29–31], in the field-free case we have already obtained estimates for the critical point and the effect of particle exchange earlier [20]. By applying the coherent anomaly extrapolation method (CAM) [32] one can extrapolate the critical exponents of the true singular behaviour and in [20] we could give a rough estimate for the exponent $\beta_n$ of the PC transition based on ($N \leqslant 6$)th order cluster GMF calculation. Now we extend the

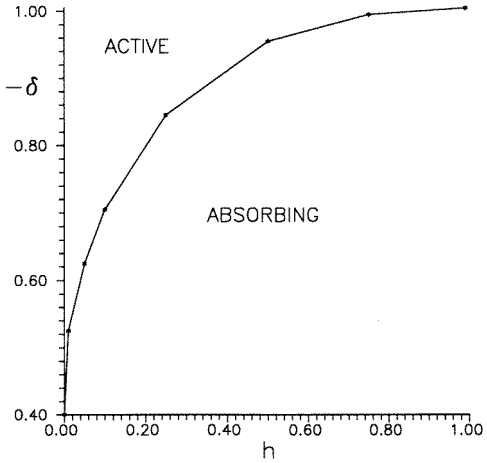


**Figure 11.** Phase diagram of NEKIM in the $(h, \delta)$ plane in the presence of an external magnetic field. Parameters of the transition probabilities: $\Gamma = 0.35$, $p_{ex} = 0.3$; see section 2. Naturally, the phase diagram can be drawn symmetrically for negative values of $h$, as well.

method for the determination of the exponent of the order-parameter fluctuation as well:

$$\chi_n(\epsilon) = L(\langle n^2\rangle - \langle n\rangle^2) \sim \epsilon^{-\gamma_n}. \tag{20}$$

The GMF equations have been set up for the steady states of NEKIM in the presence of the $H$-field. The $N$-block probabilities were determined as the numerical solution of the GMF equations for $N = 1, \ldots, 6$. The traditional mean-field solution ($N = 1$) results in stable solutions for the magnetization :

$$M = -\frac{h}{\delta} \qquad \text{if } \delta < 0 \text{ and } h^2/\delta^2 < 1 \tag{21}$$

$$= \text{sgn}(h) \qquad \text{otherwise} \tag{22}$$

and for the kink-concentration:

$$n = \frac{1}{2}\left(1 - \left(\frac{h}{\delta}\right)^2\right) \qquad \text{if } \delta < 0 \text{ and } h^2/\delta^2 < 1 \tag{23}$$

$$= 0 \qquad \text{otherwise.} \tag{24}$$

For $N > 1$ the solutions can only be found numerically. By increasing the order of approximation the critical point estimates $\delta_c(N)$ shift to more negative values similarly to the $H = 0$ case. The $\lim_{N\to\infty} \delta_c(h)$ values have been determined with quadratic extrapolation in the case of $h = 0.01, 0.05, 0.08, 0.1$. The resulting curves for $n(\delta)$ and $\chi_n(\delta)$ are shown in figures 12 and 13, respectively, for the case of $h = 0.1$ in different orders $N$ of the GMF approximation. Naturally, these curves exhibit a mean-field-type singularity at the critical point:

$$n(N) \sim \overline{\rho}_n(\delta/\delta_c(N) - 1)^{\beta_{MF}} \tag{25}$$

$$\chi_n(N) \sim \overline{\chi}_n(N)(\delta/\delta_c(N) - 1)^{-\gamma_{MF}} \tag{26}$$

with $\beta_{MF} = 1$ and $\gamma_{MF} = -1$. According to the CAM (based on scaling) the critical exponents of the true singular behaviour can be obtained via the scaling behaviour of anomaly factors:

$$\overline{n}(N) \sim \Delta^{\beta_n - \beta_{MF}} \tag{27}$$

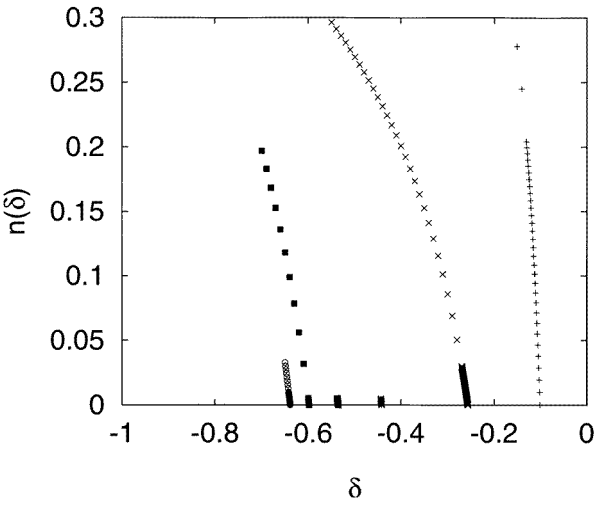


**Figure 12.** The kink density in the neighbourhood of the critical point $\delta_c(h)$ for $h = 0.1$. The curves from right to left correspond to $N = 1, \ldots, 6$ (level of GMF calculation). The points have been determined with a resolution of $10^{-5}$ in $\delta$, in order to be able to extract CAM anomaly coefficients.

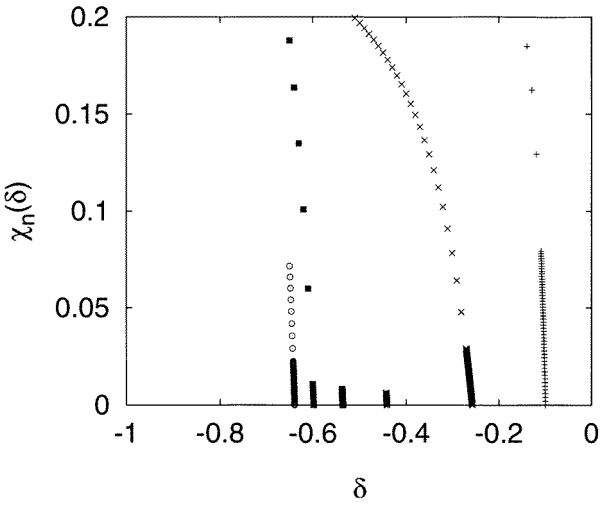


**Figure 13.** The same as figure 12 but for the second moment of the kink density. It is also apparent here that the value of $\delta_c(h)$, being equal to 0.70(1) for $h = 0.1$ according to simulations, is fairly well approximated by the GMF results for $N = 5, 6$.

$$\overline{\chi_n}(N) \sim \Delta^{\gamma_n - \gamma_{MF}} \tag{28}$$

where we have used the $\Delta = (\delta_c/\delta_c(N) - \delta_c(N)/\delta_c)$ invariant variable instead of $\epsilon$, that was introduced to make the CAM results independent of using $\delta_c$ or $1/\delta_c$ coupling [33]. Since the level of the GMF calculation which we could solve is $N \leqslant 6$, we have taken into account corrections to scaling, and determined the true exponents with a nonlinear fitting form:

$$\overline{n}_(N) = a\Delta^{\beta_n - \beta_{MF}} + b\Delta^{\beta_n - \beta_{MF}+1} \tag{29}$$

**Table 1.** CAM calculation results.

| $h$ | 0.0 | 0.01 | 0.05 | 0.08 | 0.1 | DP |
|---|---|---|---|---|---|---|
| $\beta_n$ | 1.0 | 0.281 | 0.270 | 0.258 | 0.285 | 0.2767(4) |
| $\gamma_n$ | | 0.674 | 0.428 | 0.622 | 0.551 | 0.5438(13) |

$$\overline{\chi_n}(N) = a\Delta^{\gamma_n-\gamma_{MF}} + b\Delta^{\gamma_n-\gamma_{MF}+1} \tag{30}$$

where $a$ and $b$ are coefficients to be varied. The results for various $h$'s are shown in table 1.

For $h = 0.0$ the result cited above, $\beta_n = 1.0$, has already been reported and discussed in detail in [20]. Concerning the exponent $\gamma_n$ at $h = 0.0$, we could not determine it because the low-level GMF calculations resulted in discontinuous phase transition solutions—which we cannot use in the CAM extrapolation—and so we had too few data points to achieve a stable nonlinear fitting. Higher-order GMF solutions would help, but that requires the solution of a nonlinear set of equations with more than 72 independent variables. This problem does not occur for $h \neq 0$; the above results—being based on all $N = 1 \ldots 6$ point approximations—are fairly stable.

## 5. Discussion and conclusions

Time-dependent simulations, FSS and dynamic early-time MC methods have been applied here to investigate the behaviour at and in the vicinity of a PC transition of the non-equilibrium kinetic Ising model, with the aim of completing earlier results. Emphasis has now been put on the critical properties of the 1D spin system underlying the kinks. In this way we have arrived at a more-or-less complete picture of the effect the PC transition exerts on the statics and dynamics of the 1D Ising spin phase transition. We have found that within the errors of the numerical studies the dynamic critical exponent of the kinks $Z$ and that of the spins $Z_c$ agree and have the value $Z = Z_c = 1.75$. Thus in comparison with the Glauber–Ising value $Z = 2.0$, $Z$ decreases, and so do also $\gamma$ and $\nu$: $\gamma = \nu = 0.444$ (instead of $\frac{1}{2}$). The PC point is the end-point of a line of first-order phase transitions (by keeping $p_{ex}$ and $\Gamma$ fixed and changing $\delta$ through negative values to $\delta_c$), where $\beta = 0$ still holds and also Fisher's scaling law $\gamma = d\nu - 2\beta$ is valid. The PC point has been approached from two directions: from the active phase by changing $\epsilon = \delta_c - \delta$ and from the direction of finite temperatures by varying $p_T = \mathrm{e}^{-4J/kT}$. The second moment of the magnetization (structure factor) provides the 'magnetic' exponents $x, \Theta, \gamma$, which have been found—within errors—to be twice as large as the corresponding ones for kinks, $y, \beta_n, \alpha_n$. The cause of this factor of two must lie in the nature of the active phase, of course, and it is sufficient to understand $x = 2y$ (time-dependent exponents at PC) as the rest follows from scaling relations.

The idea is to recognize that there are two characteristic growth lengths at PC which have to have the same critical exponents. Namely, the magnetic one $L(t) \propto t^x$ (see the introduction) and the cluster size defined through the square root of $\langle R^2(t)\rangle \propto t^z$. The latter is obtained by starting either from two neighbouring kink initial states (see e.g. [10]), or from a single kink [9, 11], while the magnetic domains grow in the quenching situation, i.e. from random initial states ($T = \infty \to T = 0$). Both length-exponents are, however, connected with $Z$, the dynamic critical exponent, since at PC the only dominant length is the (time-dependent) correlation length. $z/2 = 1/Z$ has been shown to follow from scaling in [9, 34] for one-kink and two-kink initial states, respectively. Presently we have found

$x = 1/Z_c$, $Z_c = Z$ within numerical errors, and thus

$$x = z/2 \tag{31}$$

follows.

Exponents of cluster growth are connected by a hyperscaling relation first established by Grassberger and de la Torre [1] for the directed percolation transition. In the same form it does not apply to the PC transition [10], where dependence on the initial state (one or two kinks) manifests itself in two cluster-growth quantities: the kink-number $N(t,\epsilon) \propto t^{\eta} f(\epsilon t^{1/\nu_\perp Z})$ and the survival probability $P(t,\epsilon) \propto t^{-\delta} g(\epsilon t^{1/\nu_\perp Z})$. (This $\delta$ has, of course, nothing to do with the parameter $\delta$ of NEKIM.) In case of systems with infinitely many absorbing states, where $\delta$ and $\eta$ depend on the density of particles in the initial configuration, a generalized scaling relation was found to replace the original relation, $2\delta + \eta = z/2$, namely [35]:

$$2(\beta_n' + \beta_n)\frac{1}{\nu_\perp Z} + 2\eta' = z' \tag{32}$$

which is also applicable to the present situation. In equation (32) $\beta_n'$ is defined through $\lim_{t\to\infty} P(t,\epsilon) \propto \epsilon^{\beta_n'}$ and the scaling relation $\beta_n' = \delta' \nu_\perp Z$ holds. A prime on the exponents indicates that they may depend on the initial state. For the PC transition the exponent $z$ seems to be independent of the initial configuration, $z' = z$.

In the case of a single-kink initial state all samples survive, thus $\delta' = 0$, and via the above scaling relation, also $\beta_n' = 0$. Equation (32) then becomes $2\beta_n/\nu_\perp Z + 2\eta' = z$. For $t \to \infty$, however, $\lim_{t\to\infty} N(t,\epsilon) \propto \epsilon^{\beta_n}$ has to hold (the steady state reached cannot depend on the initial state, provided samples survive). Thus, using the above scaling form for $N(t,\epsilon)$, $\eta = \beta_n/\nu_\perp Z$ follows and the hyperscaling law can be cast into the form

$$\frac{4\beta_n}{\nu_\perp Z} = z. \tag{33}$$

Starting with a two-kink initial state, however, $\beta_n' = \beta_n$ and $\eta' = 0$ holds [10]. With these values equation (32) again leads to equation (33).

As $z = 2/Z$, equation (34) involves—at least in the case of the PC transition—only quantities which are also defined when starting with a random initial state. Using equation (8), equation (33) becomes

$$2y = 1/Z \tag{34}$$

which, together with equation (31) leads to $2y = x$.

In this way the factor of two between magnetic and kink exponents found in this paper could be explained as following from scaling.

Finally, we have introduced a magnetic field into the NEKIM transition rates and investigated its effect mainly in the framework of generalized mean-field approximation. By going up to $(N = 6)$-order cluster approximation, the expectation that the universality class of the phase transition turns into DP type [15] has been given support: we have found values for the exponents of the kink density and its second moment which are very close to the corresponding DP values.

## Acknowledgments

The authors would like to thank Z Rácz for numerous helpful remarks and the Hungarian research fund OTKA (nos T017493 and 4012) for support during this study. The simulations were partially carried out on the Fujitsu AP1000 parallel supercomputer.

## References


[1] Grassberger P and de la Torre A 1979 *Ann. Phys.* **122** 373
[2] Cardy J L and Sugar R L 1980 *J. Phys. A: Math. Gen.* **13** L423
[3] Janssen H K 1981 *Z. Phys.* B **42** 151
[4] Grassberger P 1982 *Z. Phys.* B **47** 365
[5] Takayasu H and Tretyakov A Yu 1992 *Phys. Rev. Lett.* **68** 3060
[6] Jensen I 1993 *Phys. Rev.* E **47** R1
[7] Inui N 1993 *Phys. Lett.* A **184** 79
[8] Grassberger P, Krause F and von der Twer T 1984 *J. Phys. A: Math. Gen.* **17** L105
[9] Grassberger P 1989 *J. Phys. A: Math. Gen.* **22** L1103
[10] Jensen I 1994 *Phys. Rev.* E **50** 3623
[11] Menyhárd N 1994 *J. Phys. A: Math. Gen.* **27** 6139
[12] Zhong D and ben-Avrahamm D 1995 *Phys. Lett.* A **209** 333
[13] Kim M H and Park H 1994 Critical behaviour of an interacting monomer–dimer model *Phys. Rev. Lett.* **73** 2579
[14] Park H, Kim M H and Park H 1995 *Phys. Rev.* E **52** 5664
[15] Park H and Park H 1995 *Physica* **221A** 97
[16] Glauber R J 1963 *J. Math. Phys.* **4** 191
[17] see e.g. Kawasaki K 1972 *Phase Transitions and Critical Phenomena* vol 2 ed C Domb and M S Green (New York: Academic) p 443
[18] Droz M, Rácz Z and Schmidt J 1989 *Phys. Rev.* A **39** 214
[19] Rácz Z and Zia K P 1994 *Phys. Rev.* E **49** 139
[20] Menyhárd N and Ódor G 1995 *J. Phys. A: Math. Gen.* **28** 4505
[21] Li Z B, Schülke L and Zheng B 1995 *Phys. Rev. Lett.* **74** 3396
[22] Li Z B, Schülke L and Zheng B 1996 *Phys. Rev.* E **53** 2940
[23] Blundell R E, Hamayun K and Bray A J 1992 *J. Phys. A: Math. Gen.* **25** L733
[24] Sadiq A and Binder K 1983 *Phys. Rev. Lett.* **51** 674
[25] Milchev A, Binder K and Heermann D W 1986 *Z. Phys.* B **63** 521
[26] Menyhárd N 1990 *J. Phys. A: Math. Gen.* **23** 2147
[27] Bray A J 1994 *Adv. Phys.* **43** 357
[28] Rácz Z Private communication
[29] Gutowitz H A, Victor J D and Knight B W 1987 *Physica* **28D** 18
[30] Dickman R 1988 *Phys. Rev.* A **38** 2588
[31] Szabó G, Szolnoki A and Bodocs L 1991 *Phys. Rev.* A **44** 6375
Szabó G and Ódor G 1994 *Phys. Rev.* E **59** 2764 and references therein
[32] Suzuki M 1986 *J. Phys. Soc. Japan* **55** 4205
[33] Kolesik M and Suzuki M 1994 *Preprint* cond-mat/9411109
[34] Grassberger P 1989 *J. Phys. A: Math. Gen.* **22** 3673
[35] Mendes J F F, Dickman R, Henkel M and Marques M C 1994 *J. Phys. A: Math. Gen.* **27** 3019